Journal of Food Measurement and Characterization (2021) 15:2108–2118
https://doi.org/10.1007/s11694-020-00799-1

ORIGINAL PAPER

Fabrication and characterization of composite film based on gelatin and electrospun cellulose acetate fibers incorporating essential oil

Habib Abbasi[1] · **Hoda Fahim**[1] · **Mohaddese Mahboubi**[2]

Received: 4 November 2020 / Accepted: 30 December 2020 / Published online: 18 January 2021

Abstract

In this research, *Oliveria decumbens Vent* essential oil (OEO) at 0–45% w/w was encapsulated in cellulose acetate (CA) electrospun fibers and then incorporated in gelatin-based films. Scanning Electron Microscope (SEM) showed more uniform and compact surface in the neat gelatin film in comparison to the CA fiber loaded composite ones and microfibers were perpendicular to the fracture surface. The composites showed higher tensile strength (1.3–2.6 MPa) and lower elongation (less than 1%) than the pure gelatin film. Water solubility of the composites were significantly lower than the gelatin film (81% VS. ≈50%). The water vapor permeability (WVP) of composites was higher than the gelatin film probably due to microscopic pinholes induced by fibers, however WVP slightly decreased by increasing OEO. The contact angle values from 79.9 to 101.5° indicating increase of hydrophobicity by incorporating the CA fibers. Inhibition zones against *E. coli* and *S. aureus* (13.33 mm) confirmed the antibacterial activity of composites. It can be concluded that the composite gelatin films incorporating EO-loaded electrospun fibers could enhance the mechanical and antimicrobial properties of the composites despite increasing WVP, thus they could be potentially used for food active packaging purposes.

Keywords Active packaging · Antimicrobial activity · Cellulose acetate · Electrospinning · Gelatin · *Oliveria decumbens vent* essential oil

Introduction

In the recent years, the accumulation of residues from non-renewable and non-biodegradable sources like plastics have raised environmental concerns and led to investigate some alternative sources including proteins, polysaccharides, and lipids. Several researches on these biodegradable resources showed that these compounds are good alternatives for replacing plastics and can be successfully used as packaging materials [1]. The other attractive aspect of the bio-based packaging is their potential to incorporate a wide range of natural antimicrobial/antioxidant compounds to produce active packaging. Active packaging is a novel type of packaging which can actively protect the packaged perusable foods by releasing biologically active compounds incorporated in their structure [2].

O.decumbens essential oil (OEO) with different biological activities, has been used in treatments of ailments for decades. Several studies on *O.decumbens* essential oil (EO) confirmed its antimicrobial activity against bacteria, yeast and molds [3]. Therefore, loading EO in fiber mats to produce active packaging offers several advantages including a sustained release, prolonged effect of these active compounds and less/or no direct exposure to the food. Gelatin film coated by oleoresin-loaded-polycaprolactone electrospun fibers [2], electrospun zein-nanofiber mats loaded with curcumin to produce antifungal surface-coating application [4], and well-aligned cellulose nanofiber to reinforce polyvinyl alcohol composite film [5] are similar works in this area. Gelatin is an animal protein with a broad range of applications in food and pharmaceutical industries. This polymer is obtained from thermal denaturation of the collagen from different sources including pig, cow, fish and poultry skins

✉ Habib Abbasi
habbasi@jsu.ac.ir

Hoda Fahim
fahim.hoda@ymail.com

Mohaddese Mahboubi
Mahboubi1357@yahoo.com

[1] Department of Chemical Engineering, Jundi-Shapur University of Technology, Dezful, Iran

[2] Medicinal Plant, Research & Development, Tabib Daru Pharmaceutical Company, Kashan, Iran

and bones. Gelatin is capable to form a cohesive matrix structure, which makes it an excellent candidate for food biopackaging [6–9]. However, functional properties of gelatin films are strongly depend on the hydrophilic nature of the polymer which causes poor water resistance and mechanical properties [10]. These problems have encouraged efforts to achieve new strategies to improve the properties of gelatin films including combining the gelatin films with different polymers and/or fillers [11, 12].

Cellulose is one of the most abundant naturally occurring polymers in the world which has good thermal and mechanical stability [13]. Cellulose acetate (CA), the acetate ester of cellulose, is one of the well-known cellulose derivatives which is used in different films, fibers, and semi-permeable membranes [14]. It has been claimed that cellulose and its derivatives are able to enhance the mechanical and barrier properties of gelatin films [15]. Although the combination of carbohydrates and proteins has been widely studied, there is limit information about using of electrospun CA fibers in the protein-based films as a potentially new method to produce nanocomposite packaging films.

Electrospinning is a relatively new method to produce non-woven ultra-fine fibers. In this method, an electrode from a power supply is used to charge a viscose polymeric solution in a syringe. As a result of the electrical field, a charged jet of polymer is produced at the tip of the needle and pulled toward a cylindrical collector covered by an aluminum foil. In this the process, the polymeric solution converts to ultra-thin fibers by evaporating solvents under the electrical field between the needle and metal collector [16]. The resultant fibers bear unique characteristics such as highly porous structure and high surface-to-volume ratio which make them a good candidate for incorporating functional additives [17].

Therefore, we would expect that by incorporating OEO-loaded fibers into the film forming solution, a novel type of active composite film with enhanced antimicrobial and mechanical properties to be fabricated.

To sum up, although gelatin is an excellent film-forming material due to its abundance, low price, biodegradability and easy to be casted into film, there have some weaknesses that limit its usage including high WVP, high water solubility and low mechanical properties. Therefore, to overcome those problems, we used cellulose acetate electrospun fibers to improve their physicochemical and mechanical properties. In addition, we used electrospun fibers as a carrier to encapsulate *O.decumbens* essential oil at different levels to add antimicrobial properties into our composite films.

Material and methods

Materials

Cellulose acetate was purchased from Sigma-Aldrich Co with the average $M_n \sim 30{,}000$ by GPC and 39.8 Wt. % acetyl. Gelatin type B from bovine skin with gel strength ~ 225 g bloom was also obtained from Sigma-Aldrich Co. Extra pure acetic acid and acetone were prepared from Dr. Mojallali Chemical Industry Complex (Tehran-Iran) and used without further purification. *O. decumbens* essential oil was obtained from Tabib Daru Pharmaceutical Co (Mashhad Ardehal—Kashan -Iran). Mueller–Hinton agar and broth were purchased from Sigma-Aldrich Co.

Electrospinning

Electrospinning solutions were prepared by dissolving 12% w/w CA in acetone: acetic acid (1:2 v/v) solvent was added then the mixture was stirred at the room temperature for 5 h. The OEO was added to the solutions at different ratios of 0, 15, 25, 35 and 45% v/w (v/w with respect to the dry weight of CA polymer) and the mixture was stirred for 1 h before electrospinning. The obtained solutions were loaded into a 10-mL plastic syringe with a 22-gauge needle (0.7 mm OD × 0.4 mm ID) and pumped at a constant rate (2 mL/h). A rotating cylindrical metal (100 rpm) covered by aluminum foil was used as a collector at a distance of 7 cm from the needle tip. The applied voltage was 17 kV, and in order to achieve fiber mats with a constant thickness, the process lasted 10 h for all treatments. All samples were prepared in an electrospinning device (NanoAzma, Three Side Lab ES, Iran) at 20 °C and 50% relative humidity [18].

Film preparation

Composite films were prepared based on the previously reported method with minor modifications [19]. To put it briefly, 2 g of gelatin powder was dissolved in 100 mL distilled water at 50 °C and 20% glycerol (w/w of dry gelatin) was added to the solution. Each piece of CA fiber with the size of 6.4 × 10 mm was placed in plexiglass plates -at the same size- flatly followed by pipetting 20 mL of the gelatin solution. Each piece of CA fibers had 0.08 g weight. The samples were then dried at 40 °C in a circulating air oven (Memmert UF30m) for 24 h.

Water vapor permeability (WVP)

Barrier properties of the films against water vapor were tested according to ASTM E96-00 [20]. The film samples were tightly sealed to the cup mouths (14.15 mm ID), which they were previously filled with dry silica gels and placed in a desiccator containing distilled water at the room temperature. The cups were weighted after every 1 h intervals for up to 12 h. WVP was calculated as follow (Eq. 1):

$$WVP = \frac{Gx}{tA\Delta p} \tag{1}$$

where x is the average film thickness (m),A is the exposure area of the film (m^2), G/t is the slope of gain weight curve, and $\Delta p = P_0\left(RH_1 - RH_2\right) R_1$ and R_2 is the real water pressure difference (Pa) across the film (P_0 referred to saturated water vapor pressure at the test temperature).

Solubility in water

The solubility of the films was measured according to the previously reported method [21]. All samples were cut, weighted with 0.0001 g accuracy and placed in a circulating air oven for 24 h (105 °C). Dried films were then weighted again, followed by immersing in 30 mL distilled water for 24 h after that passed through filter papers (Whatman No.1). The filter papers with insolubilized film matters were placed in the oven for 24 h (105 °C) and weighted again. The solubility of films was calculated as Eq. (2):

$$\%FS = \frac{W_i - W_f}{W_i} \times 100 \tag{2}$$

where W_i refers to the initial weight of dry film (g), and W_f is the weight of dry insolubilized film matter.

Morphological study

The morphology of films was studied using a scanning electron microscope (SEM). Both sides of the films (rough and smooth) and the cross-section of the film with 45% EO were analyzed by TESCAN MIRAIII (Czech Republic) with a magnification of 10–50 kx. Before scanning, all samples were cut into small sizes and carefully covered by a gold layer [22].

FTIR analysis

FTIR spectrum was recorded using a spectrophotometer (Thermo Nicolet Avatar, USA). The composite films without further preparation were completely scanned at the range of 600 to 4000 cm^{-1}.

Mechanical properties

The tensile strength (TS) and elongation at break (EAB) of the films were calculated using a texture analyzer (Texture Pro. CT V1.6 Build26, Brookfield Engineering Labs, Middleboro, MA, USA) according to ASTM D882-02 [23]. In brief, all samples were cut into rectangular shape (1 × 10 cm) and conditioned in a desiccator at 25 °C and 55% RH for 3 days before the analysis. The samples were mounted between grips with initial distance of 40 mm and crosshead speed was 60 mm/min. the used load cell was 30 kg.

Contact angle measurements

The sessile dropping technique with a DSA25 Drop Analysis System (Kruss, Hamburg, Germany) was used to measure the contact angle of the films. The Millipore grade distilled water (15 µl) was used as a wetting liquid. The value of θ was measured on both sides of the droplet and averaged [24].

Antibacterial activity

The antibacterial activity of the films against *Escherichia coli* (ATCC 25,922) and *Staphylococcus aureus* (ATCC 25,923) was analyzed by the disc diffusion method [25]. Briefly, 100 µL of fresh microbial suspensions equal to 0.5 McFarland turbidity was smeared on Muller Hinton agar, then each sample was cut into a disc shape of 9 mm diameter and placed on inoculated plates and incubated for 24 h at 37 °C. The diameter of the inhibition zone was measured using the following equation (Eq. 3):

$$antibacterial\ index = \frac{area\ of\ inhibition\ zone - area\ of\ film}{area\ of\ film} \tag{3}$$

Statistical analysis

All experiments were performed in triplicate (n = 3) and a completely random design (CRD) was used. The analysis of variance (ANOVA) was done, and a means comparison was performed by Duncan test. The significant probability value was determined at P ˂ 0.05. The statistical analysis was conducted using Statistical Package for Social Science software (SPSS version 16.0).

Results and discussion

Water vapor permeability (WVP)

Our findings showed that the neat gelatin film had a significant lower WVP (around 1.08×10^{-9} (gr/pa.h.m)) compared

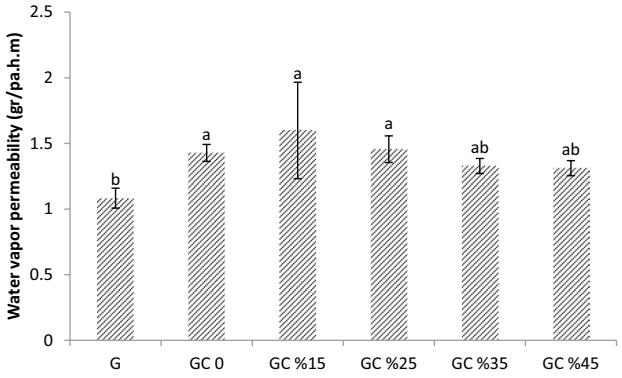

Fig. 1 The water vapor permeability of neat gelatin film; bilayer gelatin/cellulose acetate film contains 0–45% *O. decumbens* essential oil

to the composites which is similar to what reported by Carvalho et al. [26]; they reported that the WVP of *Atlantic halibut* skin gelatin was equal to 12×10^8 (gr.mm/h.cm^2.Pa). However, in our study it was observed that incorporating the CA fibers in gelatin film led to an increase in WVP. In addition, the highest water vapor permeability was observed in composite films containing 0, 15 and 25% OEO (Fig. 1) which was significantly higher than the neat gelatin film. On the other hand, an increase in the %OEO content of fibers (35 and 45%) caused a slight decrease in WVP. However, it was not significantly different from other treatments.

Water vapor permeability is mainly influenced by the hydrophilic and/or hydrophobic nature of each component, the film-forming process, the volume of the other layer and its dispersion in the film matrix, defects and cracks in film after drying, and the structural configuration of a constituent. In our study, despite the hydrophilic nature of gelatin, the neat gelatin film had the lowest WVP compared to the composites (0, 15, 25% OEO). The gelatin film showed a smooth and uniform surface without any noticeable defects, which was an indication of a more compact structure than composite films (see SEM images). It seemed that embedding electrospun fibers in the film matrix gave rise to more microscopic cracks and defects. These findings were similar to those obtained by Abdulkhani et al. [27] who investigated WVP of soy protein isolate films reinforced by CA fiber mats. The WVP reduction in composite films with 35 and 45%OEO could be related to the existence of hydrophobic OEO in the film structure. In other words, after electrospinning the solutions with higher OEO% content, the amount of remained OEO was enough to decrease WVP, although not significantly, and we believed that most of the OEO content in the solutions with lower amount (15 and 25%O EO) evaporated. Ahmad et al. [25] reported that the hydrophobic nature of essential oil incorporated in fish skin gelatin film caused a decrease in WVP, which is consistent with our results.

Solubility in water

Our results revealed that pure gelatin film dissolution in water was around 81% (Fig. 2) which was similar to other studies on gelatin film [25, 28]. Furthermore, the solubility of other samples that contained partially insoluble CA fiber mats was around 40 or 50% which was remarkably lower in comparison with gelatin film. However, there were no statistically significant differences between composite films.

The high number of polar groups in the gelatin chains makes it possible to create hydrogen bonding with water molecules. It explains the high solubility of the gelatin film in water. To be more precise, more hydrogen bonding between water and gelatin causes more solubility in the water [29]. In addition, it has been reported that the electrospinning process can alter the orientation of –OH and/or acetyl groups of CA in a way that the electrospinning makes it more hydrophobic than bulk CA [30]. This explanation would explain the solubility behavior of our composites. The addition of OEO seemed to be insignificant regarding water solubility since most of OEO evaporated during electrospining.

From the practical point of view, using biodegradable film for food packaging requires them to be resistant to water or moisture to retain their protective function during the storage. The amount of absorbed water by polysaccharide and/or protein-based films is a determinant factor to use them as a packaging material. Most of the biopolymers absorb water molecules at the first step and this process causes a change their structures and consequently change in their water solubility [31]. In our study, we noticed that the solubility of composite films was considerably decreased by embedding the electrospun structure. Indeed, the CA fibers protected the

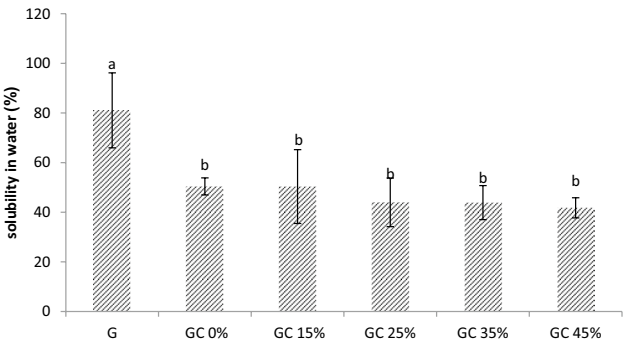

Fig. 2 Solubility in the water of neat gelatin film; bilayer gelatin/cellulose acetate film contains 0–45% *O. decumbens* essential oil

film structure during dissolution in a way that the entrapped gelatin molecule between fibers remained insoluble. These reasons can explain the less solubility of composite films in comparison to gelatin film. Reduced water solubility of laminated films has been reported in previous studies; Pereda, Ponce [32] confirmed the reduced solubility of chitosan film laminated to gelatin film (25%) layers of polylactic acid (90%) in water versus the neat gelatin film.. In addition, Rhim et al. [33] found that the solubility of soy isolated protein film laminated to three layers of polylactic acid reduced to 90% of its original weight.

Morphological study

Figure 3a and b show both sides of the neat gelatin film at two magnitudes. Both sides represented a compact surface without a porous structure without any phase separation. However, a grainy surface structure was observed on the side exposed to drying air that may be attributed to small agglomerated gelatin particles during the drying process. The dense and non-porous structure of gelatin films without any fracture has been reported in previous studies [25, 34, 35].

The surface of composite film is shown in the Fig. 3c and d. Compared with the neat gelatin film, the composite film surface became slightly rough and exhibited a wrinkled cloth structure. The film forming solution seemed infiltrated into CA-non-woven mat and filled the micropores, however the orientation of impregnated fibers retained the original characterization (Fig. 3e and f). Cai et al. [5] reported that impregnated electrospun CA fibers into which PVA resin diffused had a rougher surface than PVA film, in addition they showed that PVA filled all porous between fibers and made the composite films more transparent than electrospun fibers. Their results were in good accordance with our results (Fig. 4). The rougher surface of the composite film could be the result of diffusing and drying gelatin solution into non-woven mats, hence it shaped like the wrinkled structure of CA layer with higher surface roughness. In addition, the thickness of the films was increased by adding the cellulose acetate fibers (Figs. 5, 6 and 7).

The cross-section images of the composite film with two different magnitudes are shown in Fig. 3e and f, respectively. According to the results, the composite film was composed of two parts (Fig. 3e), the gray area was gelatin, and the spots were broken ends of CA fibers containing OEO. The porous structure of the non-woven mat facilitated the interpenetration of the gelatin biopolymer into the CA layer (Fig. 3c and d). Almost all fibers were perpendicular to the fracture surface. This is an evidence that electrospinning is able to form a film of fiber mats which are vertically aligned along the cross section of the film and individual fibers do not immerse in the polymer solution. However a few flatly layered fibers were observed on the fracture surface that might be the result of pull-out the fibers whose ends were close to the fractured surface [5]. Besides, lack of debonding between the fibers and film-forming solution as well as the rough ends of broken CA fibers in cross-section images depict a strong adherence in fiber/gelatin interface. Similar results were reported by other researchers [5, 36, 37], who observed this arrangements of fibers in epoxy, PVA, and ethylene oxide/epichlorohydrin copolymer composite films were perpendicular to fracture surface. Their findings are in good agreement with our results. Both rough broken ends and pull-out phenomena have been reported as a result of stress transfer from gelatin matrix to the fibers, means that CA fibers act as reinforcing agent in the composite film (see also tensile strength, Fig. 8b) [5, 19]. The high numbers of hydroxyl groups on the surface of CA fibers could form hydrogen-bonding interactions with hydroxyl polar groups of the gelatin. This interaction force became stronger due to the higher specific surface area of the fibers than balk CA. However, despite the good interfacial adhesion between fibers and gelatin, higher magnitude of SEM images (25 and 50 kx) depicted a small number of microscopic cracks. These cracks, although not large enough to affect the force transfer, were quite enough to influence water vapor permeability (Fig. 1) therefore we could see that WVP of the composites increased despite improving mechanical properties of the films (Figs. 1 and 8a, b respectively).

FTIR analysis

The FTIR analysis of gelatin film (Fig. 5), demonstrated a stretching absorption peak at 3291 cm^{-1} assigned to N–H amid type A, an absorption peak of about 1527 and 1621 cm^{-1} (C=O) represented amid II and amide I, respectively. Plane vibration of C-N and N–H groups related to amide bonds with $C\text{-}H_2$ of glycinin and proline side chains of gelatin at 1221 cm^{-1} was very similar to the results reported by Shahiri Tabarestani, Sedaghat [24]. They observed similar absorption peaks for fish skin gelatin films plasticized by glycerol.

The FTIR results of gelatin/CA composite film without essential oil revealed two strong and broad absorption peaks at 1100 and 1300 cm^{-1} assigned to C–O–C etheric absorption which was shifted from 1120 cm^{-1} due to the resonance. Plane vibration of C-N and N–H groups of amide bonds with $C\text{-}H_2$ (glycinin) or proline side chains of gelatin was also observed at 1226 cm^{-1}, and its shift from 1221 cm^{-1} can be explained by hydrogen bonding between CA layer and gelatin film. It appeared that in 1631 cm^{-1}, the C=O peak assigned to amide II in gelatin was overlapped by the ester peak (O=C–O) of cellulose and N–H bending vibration of amide I (gelatin). A N–H stretching vibration at 3278 cm^{-1}

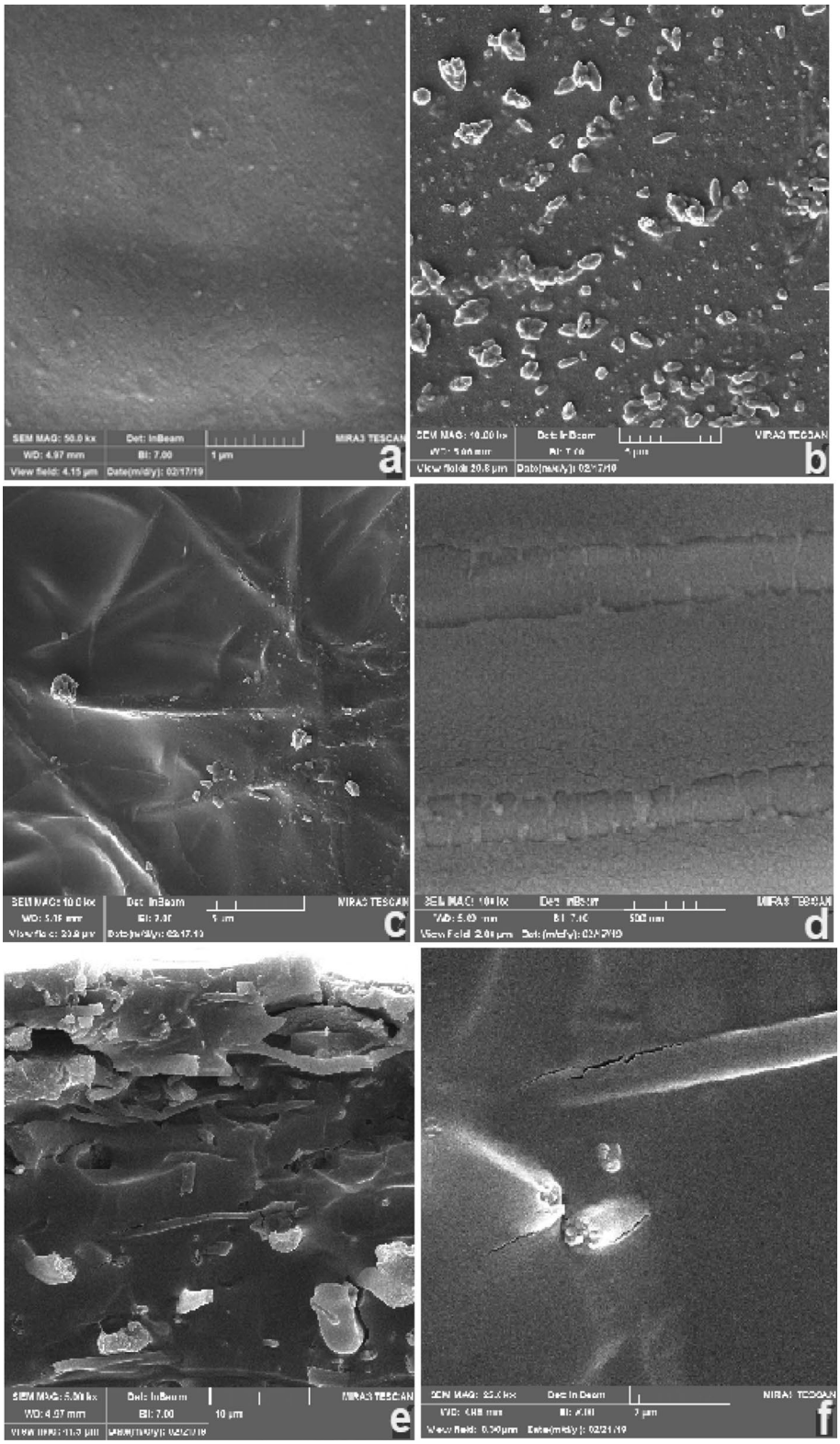

Fig. 3 SEM images of both sides of neat gelatin film (**a** and **b** respectively), CA-gelatin composite film (**c** and **d** respectively), and the cross-section of the composite film (**e** and **f**). The magnitudes were 10 kx and 50 kx

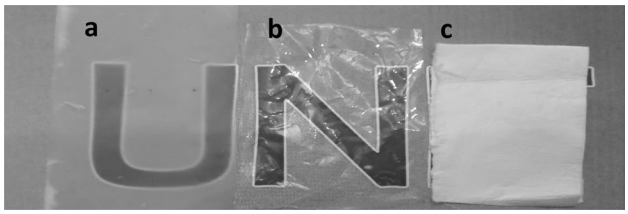

Fig. 4 **a** Bilayer film, **b** Neat gelatin film, **c** Electrospun non-woven mat sheet

of amide A of gelatin was also observed. All observed peaks were similar to previous studies [24].

A C–O–C (ether) symmetric stretching vibration was assigned to the band at 850 cm^{-1} in cellulose acetate. The sp3 C-H stretching band assigned to cellulose was observed at 2917. However, a CH_2 and CH_3 bending vibration at 1521 and 1442 cm^{-1} respectively related to cellulose acetate overlapped with stretching amide II band vibration. Liakos et al. [38] reported that the C=O ester band of cellulose acetate appeared at around 1750 cm^{-1}, which was similar to our absorption peak.

The FTIR spectrum of composite film containing 45% essential oil showed absorption peaks as follow: a peak attributed to non-aromatic ring (γ-terpinene) overlapped with an amide band was observed at 1632 cm^{-1}. Two sharp peaks should have existed in the range of 1400 to 1600 cm^{-1} assigned to aromatic rings (all essential compounds exclude γ-terpinene) have been overlapped with shifted bending vibration of cellulose acetate (1443 and 1529 cm^{-1} respectively). This might have shown hydrogen bonding between cellulose acetate and essential oil. Other peaks in the spectrum were similar to the composite film without essential oil. The slight differences between peaks may be related to hydrogen bonds between the essential oil compounds and gelatin/CA film. The Aromatic compounds in the *O. decumbens* EO, including carvacrol (a phenolic oxygenated monoterpene), thymol (a phenolic monoterpene), p-cymene (a monoterpene $C_{10}H_{14}$) as well as γ-terpinene, a non-aromatic monoterpene compound, have been reported in previous studies [3, 39]. The peaks appeared at 812 cm^{-1}, and 1632 cm^{-1} were assigned to the para, and gamma compounds, respectively. However, γ-terpinene and p-cymene are biological precursors of thymol. The thymol is also an isomeric form of carvacrol [40]. Different absorption peaks

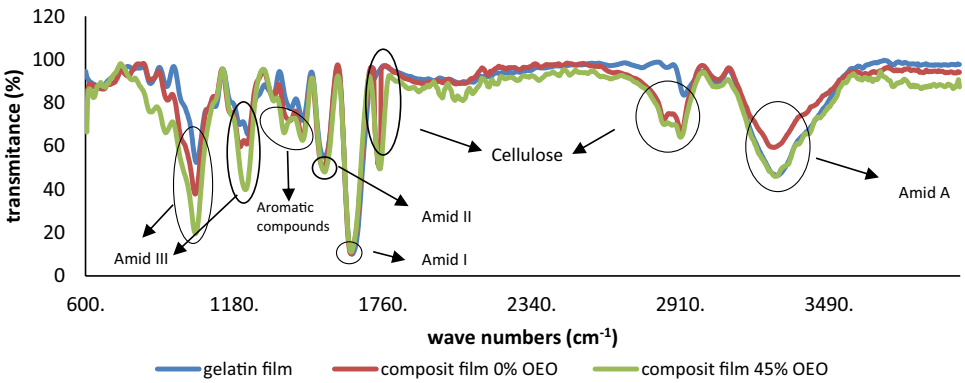

Fig. 5 FTIR analysis of neat gelatin film, bilayer gelatin/cellulose acetate film contains 0 and 45% *O. decumbens* essential oil (the blue line: gelatin film, the red line: gelatin/cellulose acetate film 0%, the green line: gelatin/cellulose acetate film 45%)

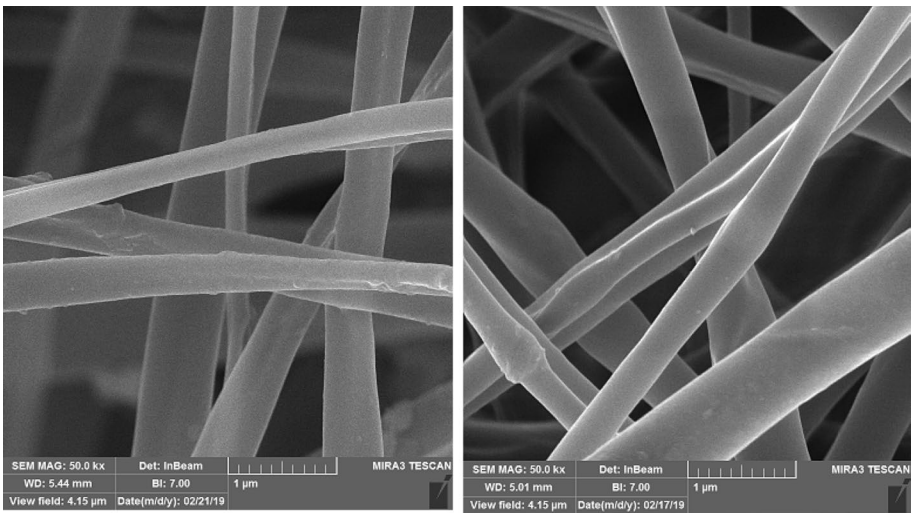

Fig. 6 SEM images of CA fibers (left 0%, right 45%)

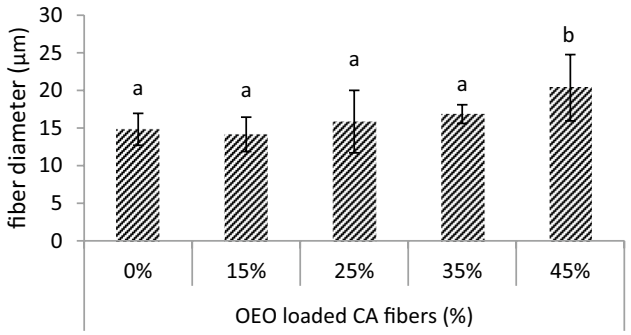

Fig. 7 Fibers diameters containing 0–45% *O. decumbens Vent* essential oil

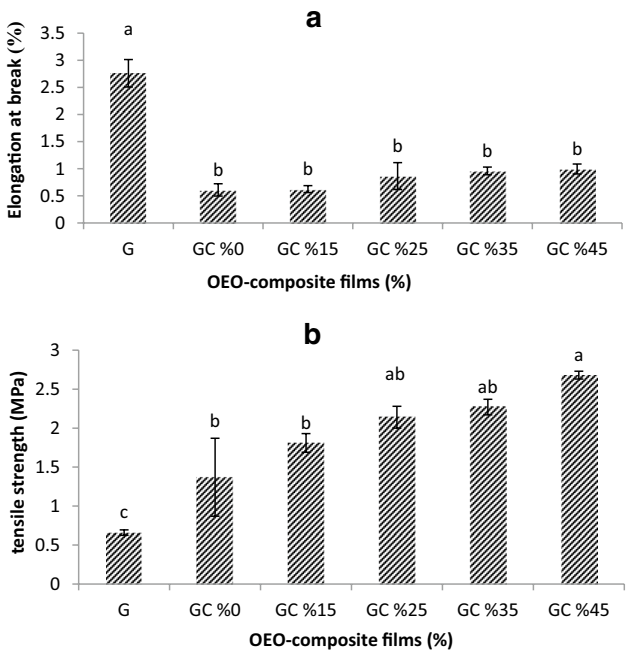

Fig. 8 **a** The Elongation at break, **b** the tensile strength of neat gelatin film and the composite gelatin/cellulose acetate film contains 0–45% *O. decumbens* essential oil

in the FTIR spectrum confirmed that the essential oil was entrapped in electrospun structure. In comparison with the composite film without OEO, some shifts that appeared in the composite containing OEO peaks may represent hydrogen bonding between volatile compounds and cellulose acetate functional groups. These findings are perfectly matched with those reported by Liakos et al. [38], Kamal [41].

In general, when a fiber mat is added to a gelatin film, the peak absorption intensity of amide A at 3200 to 3300 cm^{-1} regions is significantly lowered. This maybe the result of less hydrated chains of gelatin as a result of water molecules absorbed by CA fibers [42].

Mechanical properties

Figure 8a and b showed elongation at break (EAB) and tensile strength (TS) of films, respectively. The effect of the CA layer on EAB was inevitable, as the neat gelatin film had the highest EAB among samples and there was no significant difference between composite films ($p < 0.05$). It seemed that the electrospun structure in gelatin film significantly decreased the tensile properties of films ($p < 0.05$), while the amount of OEO in fibers had no significant effect on EAB values. This could be due to the fact that during electrospinning process and solvents evaporation, some amount of OEO evaporated and the residual amount played no important role in EAB. This result was aligned with our antimicrobial test (Table 1). The EAB of films was controlled by the CA as its value for the neat gelatin film was 2.76%; this was approximately 4 times that of composite films. In the gelatin film, glycerol as a plasticizer acting as a lubricant between protein chains and increase the film elasticity [24]. Although glycerol was used in the formulation of composite films, the strengthening effect of the electrospun layer was more pronounced than the plasticizing effect of glycerol. On the other hand, the TS of gelatin film was remarkably lower than composites; however, the TS got increased when the essential oil increased from 0 to 45% (1.37 and 2.68 MPa, respectively). Contrary to EAB, the tensile strength seemed to be affected by the amount of OEO (Fig. 8b). This may be related to the increasing fiber diameter because of an increase in OEO content in the electrospun solution (Figs. 6 and 7). Owing to the fact that an increase in %OEO content in the electrospining solution may results in lower conductivity and consequently decrease the electricity at the tip of needle, the fibers with higher diameter are produced [43]. Based on the results of Zhang and Hsieh [44], electrospun fibers with higher mean diameter had higher mechanical strength than

Table 1 Inhibition zones of neat gelatin film; and bilayer films containing different concentrations of *O. decumbens* EO against *E. coli* and *S. aureus*

Treatment	Inhibition zone (mm)	
	E. coli	*S. aureus*
Neat gelatin	0^{d}	0^{c}
%0 GC	0^{d}	0^{c}
%15 G/C	0^{d}	0^{c}
%25 GC	11 ± 1^{c}	12.33 ± 0.57^{b}
%35 GC	12.33 ± 0.57^{b}	13 ± 1^{b}
% 45 GC	13.33 ± 0.57^{b}	13.33 ± 1.52^{b}
Pure OEO	21.1 ± 0.61^{a}	31 ± 0.68^{a}

Values are the mean ± standard deviation of triplicates. Mean with different letters in indicating a significant difference between treatments ($P < 0.05$)

those with lower diameter; their results were in accordance with our results. Furthermore, during the tensile test, the uniaxial orientation of CA fibers positively affected the force transferring to composite film. This means that the CA fibers acted as a bridge in the gelatin matrix and prevented defects and cracks induced by tensile strength. Similar results are reported by Chen and Liu [19] who studied soy protein films reinforced by electrospun cellulose nanofibers. Wang et al. [45] also revealed that a montmorillonite/chitosan-poly (ethylene oxide) nanofibrous membrane could enhance mechanical properties of poly (vinyl alcohol-co-ethylene) composite film.

The mechanical properties of the composite films depend on several factors including adhesion and compatibility between polymer matrix and reinforcing agent (i.e., CA fibers), stress transfer efficiency due to reinforcing agent, the volume ratio and the aspect ratio of reinforcing agent, the direction of the fibers and the degree of crystallinity of the film matrix [46]. In our study, the direction of fibers was parallel to the force direction. In all samples, the size and weight of the electrospun fibers were the same and there was a good adhesion between two layers. These findings are in good agreement with Abdulkhani et al. [27]; they reported that most of the fibers were parallel to the direction of applied load and there was high-stress transfer efficiency which in turn led to a noticeable decrease in EAB and an increase in TS.

Contact angle measurements

The results presented in Fig. 9 shows that our composite films have moderate wettability with contact angles from 79.9 to 101.5°. According to our results, the contact angle was affected by both gelatin and CA fibers as well as the essential oil content ($p < 0.05$). The hydrophilic nature of gelatin led to the reduction of contact angle; however, it is worth noting that despite the hydrophilic nature of bulk CA, electrospun CA fibers showed a less hydrophilic property. Therefore, the composite films had significantly higher contact angle compared to gelatin film. Thakur et al. [30] reported that the above-mentioned difference could be attributed to the different orientation of the functional groups on the surface of electrospun fibers. It is worth remembering that CA contains both hydrophilic and hydrophobic molecules, -namely OH and $–CH_3COO$ groups respectively, and after electrospinning of CA solution, the orientation of acetyl groups on the surface of fibers make it more hydrophobic than bulk CA [30]. Taking into account the classification of contact angle method, contact angle ranging from 0 to 90° implicates the "wettable" surface of the film, whilst a 90–180° range of contact angle demonstrates a "partly lipophilic" film surface [47]. Neat gelatin film showed the most hydrophilic surface with the contact angle around 79.9° classified as "wettable". It is well-known that most essential oils are non- or less-polar molecules with a lipophilic nature [48], therefore, incorporating the OEO into the fibers that creates hydrogen bonding with CA fibers, might presumably lead to less hydrophilic surface of the films. Based on Sahraee et al. [47] report, adding 0.3 g/g or less of corn oil to gelatin-based nanocomposite films reduced the wettability of the film surface.

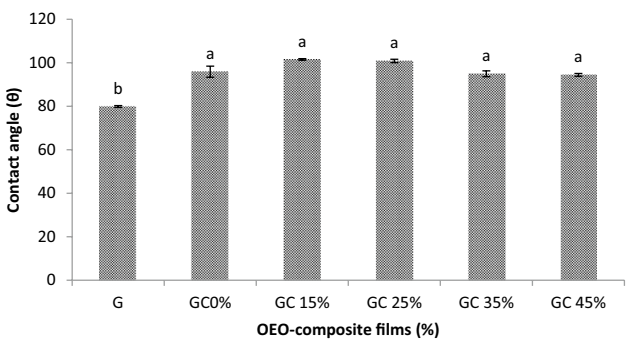

Fig. 9 The contact angle of neat gelatin film; bilayer gelatin/cellulose acetate film contains 0, 15, 25, 35 and-45% *O. decumbens* essential oil

Antibacterial activity

Our results showed that gelatin film and bilayer film without OEO had no antibacterial properties (Table 1). The inhibition zone diameter against *E. coli* increased with increasing the %OEO in a dependent manner. The highest inhibition zone was observed in films containing 35 and 45% OEO, approximately around 12.33 and 13.33 mm, respectively. However, there was no significant difference between different %OEO-loaded films. The similar results were found for *S. aureus* and although there was no observed pronounced difference, the inhibition zone increased from 12 to 13.3 mm for 15 and 45%OEO incorporated films, respectively.

In general, our findings represented a slightly higher antibacterial activity against *S. aureus*. Similarly, Amin et al. [49], Esmaeili et al. [50], and Hojjati and Ghodsi [3] reported that the main components of the *O. decumbens* EO were thymol (26.9%), carvacrol (25%), p-cymene (13.3%), and γ-terpinene (11%). Our FTIR results also confirmed the presence of OEO in CA fibers and the antibacterial test, in turn, revealed its antimicrobial activity. In addition, Hojjati et al. [3] reported that the antibacterial effect of the OEO was higher against G^+ bacteria rather than G^- which was in accordance with our results (Table 1).

Electrospun fibers can be used as a novel encapsulating agent for bioactive compounds like OEO. High aspect ratio, micro or nano-sized pores, and high porosity are the main characteristics through which the fibers can perfectly play

their carrier role for drug delivery and controlled release of loaded drugs or nutrients [51]. OEO-loaded fibers have been investigated by several researchers [52–54]. In our research pure OEO inhibition zone against *E. coli* and *S. aureus* was 21 and 31 mm respectively, while composite film containing 45% considerably had lower activity against mentioned bacteria. These results could be explained by the low solubility of the CA layer. The high concentration of encapsulated OEO in fibers could not be released in a short time, thus the CA layer swelled slightly inside the agar medium, therefore the inhibition zones around film discs were not clear and hardly detectable. In this regard, Liakos et al. [38] reported that three different OEO incorporated in CA fibers represented an unclear inhibition zone, which was consistent with our results.

Conclusion

In the current study, a composite gelatin/CA active packaging film with higher mechanical properties and antimicrobial activity was produced by incorporation EO–loaded fibers into gelatin-based films. The resultant films with 35 and 45% of essential oils had 13.33 mm of inhibition zones against *E. coli* and *S. aureus*. CA non-woven mat decreased the water solubility of the composite films because of different orientation of OH and/or acetyl groups on the fiber surfaces. However due to some cracks and pinholes induced by incorporation of fibers, WVP of the composite films increased. On the contrary, increasing OEO content in the CA fibers slightly decreased the WVP of composite films. Neat gelatin film showed the lowest contact angle while by adding the CA fibers and OEO content this parameter increased.

Our results suggested that by incorporating 45% EO into CA electrospun fibers, the mechanical properties and water resistant of the composite films improved and those films could effectively inhibit bacterial growth. Our results showed these kind of composite films can be used as new film packaging material for food industrial purposes.

Funding This work was supported by the Jundi-Shapur University of Technology, (Project No. 96–2-395–02).

Compliance with ethical standards

Conflict of interest The authors declare that there are no conflict of interest.

References

1. A. Abedinia, F. Ariffin, N. Huda, A.M. Nafchi, Int. J. Biol. Macromol. **109**, 855 (2018)
2. K.J. Figueroa-Lopez, J.L. Castro-Mayorga, M.M. Andrade-Mahecha, L. Cabedo, J.M. Lagaron, Nanomaterials **8**(4), 199 (2018). https://doi.org/10.3390/nano8040199
3. M. HojjatiM. Ghodsi. in 2nd International and 6th National Conference of Organic vs. Conventional Agriculture. Iran. (2019)
4. A. Yilmaz, F. Bozkurt, P.K. Cicek, E. Dertli, M.Z. Durak, M.T. Yilmaz, Innov. Food Sci. Emerg. Technol. **37**, 74 (2016). https://doi.org/10.1016/j.ifset.2016.08.008
5. J. Cai, J. Chen, Q. Zhang, M. Lei, J. He, A. Xiao, C. Ma, S. LiH, Xiong, , Carbohydr. Polym. **140**, 238 (2016). https://doi.org/10.1016/j.carbpol.2015.12.039
6. Y. Alparslan, J. Food Meas. Charact. **12**(1), 317 (2018)
7. Z. Didar, J. Food Bioproc. Eng. **2**(2), 113 (2019)
8. A. Tügen, B. OcakÖ. Özdestan-Ocak, J. Food Meas. Charact. 1 (2020).
9. A. Abedinia, A.M. Nafchi, M. Sharifi, P. Ghalambor, N. Oladzadabbasabadi, F. Ariffin N. Huda, Trends Food Sci. Technol. (2020).
10. S.N. Syahida, M.R. Ismail-Fitry, Z.M.A.A. Ainun, Z.A.N. Hanani, Food Packag Shelf Life. **23**, 100437 (2020). https://doi.org/10.1016/j.fpsl.2019.100437
11. K. Li, S. Jin, H. Chen, J. Li, Compos. B. Eng. **171**, 222 (2019)
12. Y. Wang, R. Zhang, W. Qin, J. Dai, Q. Zhang, K. Lee, Y. Liu, Mater. Design. **185**, 108277 (2020)
13. D. HaldarM.K. Purkait, Carbohydr. Polym.116937 (2020).
14. C.C. Pola, E.A. Medeiros, O.L. Pereira, V.G. Souza, C.G. Otoni, G.P. Camilloto, N.F. Soares, Food Packag. Shelf Life. **9**, 69 (2016). https://doi.org/10.1016/j.fpsl.2016.07.001
15. H.M. Azeredo, M.F. Rosam, L.H. Mattoso, Ind. Crops Prod. **97**, 664 (2017). https://doi.org/10.1016/j.indcrop.2016.03.013
16. B. Pant, M. ParkS.-J. Park, , Pharm. **11**(7), 305 (2019)
17. D.A. Schmatz, J.A.V. Costa, M.G. de Morais, Food Packag. Shelf Life. **20**, 100314 (2019). https://doi.org/10.1016/j.fpsl.2019.100314
18. M.M. Mehanna, Int. J. Pharm. Investig. **10**(1), 82 (2020)
19. G. ChenH, Liu, , J. Appl. Polym. Sci. **110**(2), 641 (2008). https://doi.org/10.1002/app.28703
20. ASTM, Standard Test Methods for Water Vapor Transmission of Materials. Standard designation E96 / E96M-16, in Annual Book of ASTM Standards. 2016, ASTM International: West Conshohocken, PA,.
21. M. Rezaei, A. Motamedzadegan, World J. Nano Sci. Eng. (2015). https://doi.org/10.4236/wjnse.2015.54019
22. K.M. Soto, M. Hernández-Iturriaga, G. Loarca-Piña, G. Luna-Bárcenas, C.A. Gómez-Aldapa, S. Mendoza, J. Food Sci. Technol. **53**(10), 3787 (2016). https://doi.org/10.1007/s13197-016-2365-y
23. ASTM, Standard test method for tensile properties of thin plastic sheeting. Standard designation D882–18, in In Annual Book of ASTM Standards. 2018, American Society for Testing and Materials: West Conshohocken, PA, 2018.
24. H. Shahiri Tabarestani, N. Sedaghat, M. Jahanshahi, A. Motamedzadegan, M. Mohebbi, J Aquat. Food Produc. Technol. **26**(10), 1244 (2017). https://doi.org/10.1080/10498850.2015.1126664
25. M. Ahmad, S. Benjakul, T. Prodpran, T.W. Agustini, Food Hydrocoll. **28**(1), 189 (2012). https://doi.org/10.1016/j.foodhyd.2011.12.003
26. R. Carvalho, P. Sobral, M. Thomazine, A. Habitante, B. Giménez, M. Gómez-Guillén, Montero. Food Hydrocoll. **22**(6), 1117 (2008). https://doi.org/10.1016/j.foodhyd.2007.06.003

27. A. Abdulkhani, J. Hosseinzadeh, A. Ashori, S. Dadashi, Z. Takzare, Polym Test. **35**, 73 (2014). https://doi.org/10.1016/j.polymertesting.2014.03.002
28. R.J. Shakila, E. Jeevithan, A. Varatharajakumar, G. Jeyasekaran, D. Sukumar, Food Chem. **135**(4), 2260 (2012). https://doi.org/10.1016/j.foodchem.2012.07.069
29. Z.N. Hanani, Y. Roos, J.P. Kerry, Food Hydrocoll. **29**(1), 144 (2012). https://doi.org/10.1016/j.foodhyd.2012.01.015
30. N. Thakur, A. Sargur Ranganath, K. Sopiha, A. Baji, ACS Appl. Mater. Interfaces. **9**(34), 29224 (2017). https://doi.org/10.1021/acsami.7b07559
31. K.Y. Lee, J. Shim, H.G. Lee, Carbohydr. Polym. **56**(2), 251 (2004). https://doi.org/10.1016/j.carbpol.2003.04.001
32. M. Pereda, A. Ponce, N. Marcovich, R. Ruseckaite, J. Martucci, Food Hydrocoll. **25**(5), 1372 (2011). https://doi.org/10.1016/j.foodhyd.2011.01.001
33. J.-W. Rhim, J.H. Lee, P.K. Ng, LWT-Food Sci. Technol. **40**(2), 232 (2007). https://doi.org/10.1016/j.lwt.2005.10.002
34. S.F. Hosseini, M. Rezaei, M. Zandi, F. Farahmandghavi, Food Hydrocoll. **44**, 172 (2015). https://doi.org/10.1016/j.foodhyd.2014.09.004
35. P. Tongnuanchan, S. Benjakul, T. Prodpran, Food Hydrocoll. **41**, 33 (2014). https://doi.org/10.1016/j.foodhyd.2014.03.015
36. H. Liao, Y. Wu, M. Wu, X. Zhan, H. Liu, Cellulose **19**(1), 111 (2012). https://doi.org/10.1016/j.foodhyd.2014.03.015
37. D.A. Stone, N.D. Wanasekara, D.H. Jones, N.R. Wheeler, E. Wilusz, W. Zukas, G.E. Wnek, L. Korley, ACS Macro Lett. **1**(1), 80 (2012). https://doi.org/10.1021/mz200049v
38. I. Liakos, L. Rizzello, H. Hajiali, V. Brunetti, R. Carzino, P. Pompa, A. Athanassiou, E. Mele, J. Mater. Chem. B. **3**(8), 1583 (2015). https://doi.org/10.1039/C4TB01974A
39. H. Sereshti, Y. Izadmanesh, S. Samadi, J. Chromatogr. A. **1218**(29), 4593 (2011). https://doi.org/10.1016/j.chroma.2011.05.037
40. J.B. Custódio, M.V. Ribeiro, F.S. Silva, M. Machado, M.C. Sousa, J. Exp. Pharmacol. **3**, 69 (2011). https://doi.org/10.2147/jep.s16387
41. H. Kamal, J. Radiat. Res. Appl. Sci. **7**(2), 146 (2014). https://doi.org/10.1016/j.jrras.2014.01.003
42. I. Yakimets, N. Wellner, A.C. Smith, R.H. Wilson, I. Farhat, J. Mitchell, Polym. **46**(26), 12577 (2005). https://doi.org/10.1016/j.polymer.2005.10.090
43. C. Yang, X. Wu, Y. Zhao, L. Xu, S. Wei, J. Appl. Poly. Sci. **121**(5), 3047 (2011). https://doi.org/10.1002/app.33934
44. L. Zhang, Y.-L. Hsieh, J. Nanosci. Nanotechnol. **8**(9), 4461 (2008). https://doi.org/10.1166/jnn.2008.285
45. P. Wang, H. Wang, J. Liu, P. Wang, S. Jiang, X. Li, S. Jiang, Carbohydr. polym. **181**, 885 (2018). https://doi.org/10.1016/j.carbpol.2017.11.063
46. A. Dufresne, D. Dupeyre, M. Paillet, J. Appl. Polym. Sci. **87**(8), 1302 (2003). https://doi.org/10.1002/app.11546
47. S. Sahraee, J.M. Milani, B. GhanbarzadehH, Hamishehkar. LWT-Food Science. Technology. **76**, 33 (2017). https://doi.org/10.1016/j.lwt.2016.10.028
48. A. Ait-Ouazzou, L. Cherrat, L. Espina, S. Lorán, C. Rota, R. Pagán, Innov. Food Sci. & Emerg. Technol. **12**(3), 320 (2011). https://doi.org/10.1016/j.ifset.2011.04.004
49. G. Amin, M.H.S. Sourmaghi, M. Zahedi, M. Khanavi, N. Samadi, Fitoterapia **76**(7), 704 (2005). https://doi.org/10.1016/j.fitote.2005.06.009
50. H. Esmaeili, A. Karami, F. Maggi, J. Clean. Prod. **198**, 91 (2018). https://doi.org/10.1016/j.jclepro.2018.07.029
51. W. Cui, Y. Zhou, J. Chang, Sci. Technol. Adv. Mater. **11**(1), 014108 (2010). https://doi.org/10.1088/1468-6996/11/1/014108
52. K.A. Rieger, J.D. Schiffman, Carbohydr. polym. **113**, 561 (2014). https://doi.org/10.1016/j.carbpol.2014.06.075
53. C.L. Mori, N.A.D. Passos, J.E. Oliveira, T.F. Altoé, F.A. Mori, L.H.C. Mattoso, J.R. Scolforo, G.H.D. Tonoli, J. Nanomater. **16**(1), 33 (2015). https://doi.org/10.1155/2015/439253
54. P. Wen, D.-H. Zhu, H. Wu, M.-H. Zong, Y.-R. Jing, S.-Y. Han, Food Control **59**, 366 (2016). https://doi.org/10.1016/j.foodcont.2015.06.005